Near-Field (NF) Measurements and Statistical Analysis of Random Electromagnetic (EM) Fields of Antennas and Other Emitters to Predict Far-Field (FF) Pattern Statistics

Barry J. Cown
Director, GEMTECH Microwaves, llc
2636 Caisson Court NW
Marietta GA 30064-1206
bjcown@yahoo.com

John P. Estrada
Director, Microwave Vision Group USA (MVG-USA)
2105 Barrett Drive, Suite 104
Kennesaw, GA 30144
john.estrada@mvg-usa.com

***Abstract*—This paper discusses the application of modern NF measurements and statistical analysis techniques to efficiently characterize the FF radiation pattern statistics of antennas and other EM emitters whose radiated EM fields vary erratically in a seemingly random manner. Such randomly-varying radiation has been encountered, for example, in measurements involving array antenna elements and reflector feed horn(s) containing active or passive devices that affect the relative phases and/or amplitudes of the pertinent RF signals in a non-deterministic manner [1-7]. In-Band (IB) as well as Out-Of-Band (OB) signals may be involved in some cases. Other possible randomly varying EM radiations of interest include leakage from imperfectly-shielded equipment, connectors, cables, and waveguide runs [8-9]**

I. INTRODUCTION

Previous work at GTRI [1-5,7] and at GEMTECH Microwaves (+) llc, [4]) involving coherent CW frequency domain measurements of randomly varying complex NF electric fields has shown that valid computations of key FF radiation pattern statistics can be achieved by making the appropriate Near-Field to Far-Field (NF-FF) transformations of the following measurement-derived quantities: a) the sample average value of the complex electric field at each NF measurement point, b) the sample average value (*a real number*) of the standard deviation or variance of the complex electric field at each NF measurement point, and c) the sample average values of the complex cross-covariance functions at all different NF measurement points.

The key FF radiation pattern statistics of most interest are typically a) the statistical average FF radiation pattern, b) the standard deviation or variance, c) the probability density function (p.d.f.), and d) the Cumulative Probability Distribution (C.P.D.) from which all higher order statistical moments of interest can be calculated.

The NF cross-covariance functions introduce a new level of complexity in NF measurements and analysis that is absent for "deterministic" EM field measurements because the cross covariance functions must be derived from the measured data for all different NF measurement points on the NF surface in order to compute valid Pattern FF statistics. However, MST arrays can be used to great advantage to achieve tolerable NF measurement times for the cross covariance functions and the aforementioned NF statistical quantities, thereby enabling succinct EMC characterizations of FF pattern statistics.

II. PRIMARY OBJECTIVES AND SCOPE

The primary objectives of this paper are to examine the NF data measurement and statistical processing requirements to predict the FF pattern statistics for antennas whose radiated fields vary erratically in a seemingly random manner. The scope of this paper is focused primarily on *coherent CW frequency domain measurements* at in-band (IB) or out-of-band (OB) frequencies for which a reliable phase reference is available throughout the entire NF measurement process. We note that a novel *time domain* approach for measuring random emissions from equipments has been developed by researchers at SUPELEC [8,9].

III. ORGANIZATION OF PAPER

The remainder of this paper is organized as follows. The results of analyses and numerical simulations of a randomly-phased wire dipole array antenna to examine the significance of NF covariance functions on the FF pattern statistics are summarized in Subsection IV.A and IV.B. Concluding remarks are contained in Section V. A list of references is included at the end of this paper.

IV. WIRE DIPOLE ARRAY

IV.A. NF MEASUREMENT SIMULATIONS

Measurement simulations were performed for the array of nine center-fed, vertically-oriented dipoles shown in Figure 1 in order to gain insight into the role of NF covariance functions on FF pattern statistics. The array is fed by a constant voltage source and a phase shifter controls the relative phase of the RF signal in each element. The voltage phase shifts are independent identically distributed (*i.i.d.*) random variables that each follow a Gaussian distribution with zero mean and a standard deviation of 1.0 radian. All other RF and physical characteristics of the feed structure do not vary randomly and are not taken into account in the following analysis. A sketch of the simulated NF measurement situation is shown in Figure 1.

A plot of the deterministic, non-random, relative power versus transverse distance along the NF measurement line is shown in Figure 2 for the in-band design frequency of 3.0 GHz. The NF data were computed for 65 measurement points along the transverse line spanning a total length of $8\lambda_0$, where λ_0= wavelength at 3.0 GHz. Simulations were also performed for the out-of–band (OB) third harmonic frequency of 9.0 GHz. The requisite sample average values of the complex electric field and the variance at each NF sample point and the cross-covariance values at all other NF sample points were obtained by averaging the results of 50 "Monte Carlo" runs. (The Monte Carlo runs are not included herein due to space limitations.)

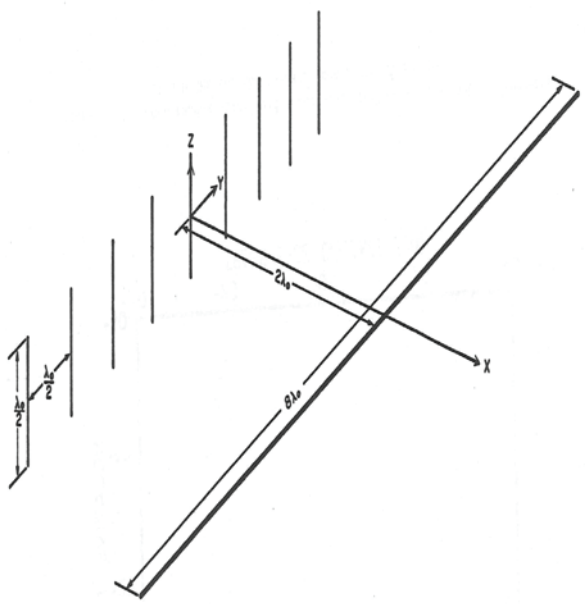

Figure 1. NF measurement geometry for wire dipole array.

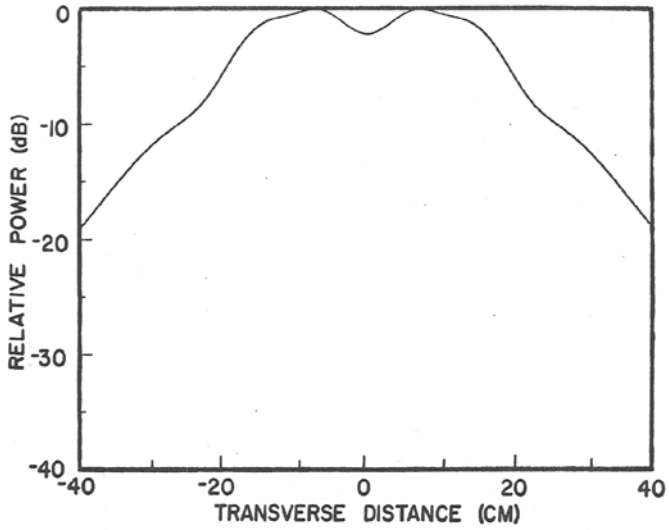

Figure 2. Deterministic Relative Power versus transverse distance along measurement line for 3.0 GHz

IV.B. KEY RESULTS

VI.B.1. NF COVARIANCE FUNCTIONS

The salient aspects of the NF covariance simulations can be summarized with the aid of Figures 3 and 4 for the in-band 3.0 GHz frequency and the third harmonic 9.0 GHz out-of-band frequency, respectively. Each figure contains a plot labeled "total" covariance and another plot labeled "intrinsic" covariance. The intrinsic covariance is the NF covariance that would be observed for the

electric fields radiated by *isolated* current elements in the absence of any mutual coupling among the radiating elements. The total covariance function includes the effects of mutual coupling which cause the element currents to be correlated.

Inspection of the NF total and intrinsic covariance functions plotted in Figure 3 shows that the total covariance and intrinsic covariance functions for 3.0 GHz differ noticeably, and the peak magnitude of the total covariance function is about 2. 7 dB greater than the intrinsic covariance peak. This result is expected because the radiating current element correlations manifest themselves in producing stronger NF covariances than would exist for isolated, non-interacting elements.

Also note that the peak magnitudes of the total and intrinsic NF covariances for 9.0 GHz frequency are significantly weaker than for 3.0 GHz and that the intrinsic and total NF covariances differ only slightly. These behaviors are expected because the inter-element spacing in terms of wavelength is much greater for 9.0 GHz than for 3.0 GHz and, hence, the inter-element mutual coupling is correspondingly weaker than for 3.0 GHz. These trends in the NF covariance functions also manifest themselves in the behavior of the FF pattern statistics, as discussed in the next section.

IV.B.2 Retrieval of NF Covariance Functions

It is possible to obtain useful estimates of the current covariance functions by applying linear operator theory and techniques to define the matrix relating element source currents to the measured NF covariance functions. The matrix is then solved by using the measured NF covariance functions as the known right-hand column vector. The matrix is nearly singular but it can be solved by applying Tanabe's projection method or other solution methods that are designed to solve nearly-singular matrices [11]. Plots of the exact and retrieved current covariances are shown in Figure5.

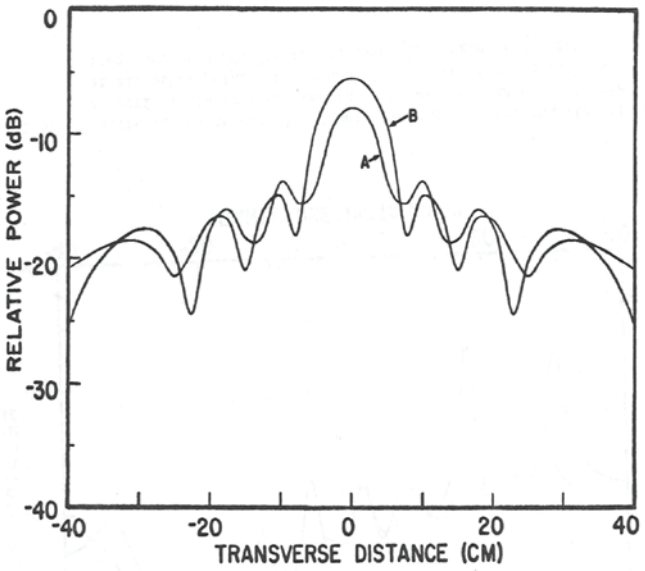

Figure 3. NF covariance function $C_{q'q}$ for E(q=0) and E^* at all other NF measurement points for randomly-phased dipole array of Fig 1, for in-band design frequency = 3.0 GHz. A=Intrinsic, B= Total

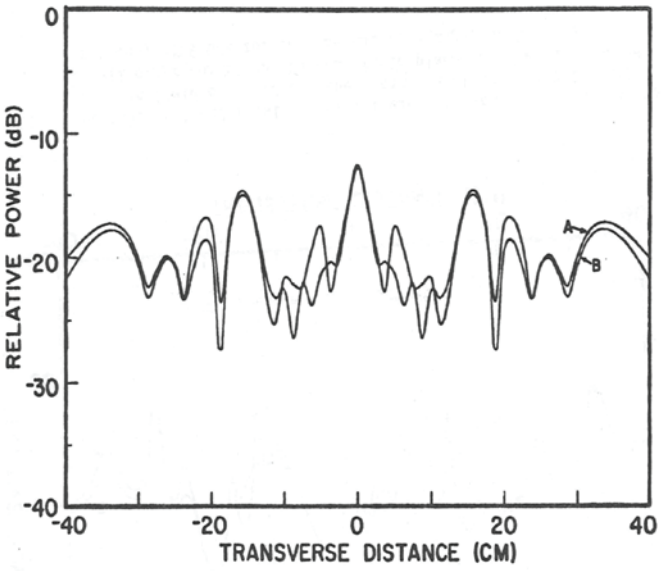

Figure 4. **NF covariance function $C_{q'q}$ for E(q=0) and E^* at all other NF measurement points for randomly-phased dipole array of Fig 1, for the out-of-band frequency of 9.0 GHz. A=Intrinsic, B= Total,**

The exact and retrieved current covariances were then used to compute the NF covariance functions displayed in Figure 6. The retrieved NF covariance function agrees reasonably well with the exact function and may provide useful engineering estimates for some purposes. Further investigations

are needed to assess the overall utility and accuracy of this technique for real-world antenna applications.

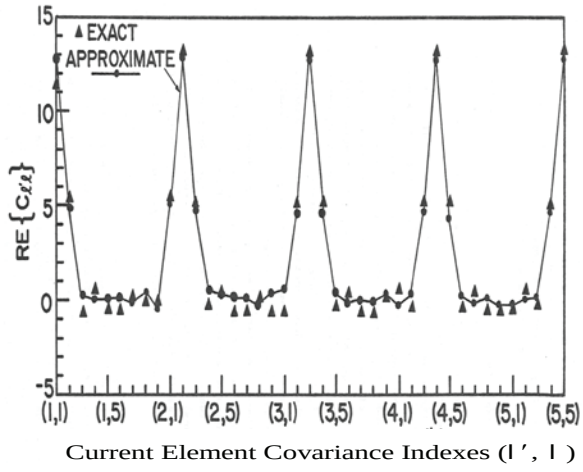

Figure 5. Element Covariance Functions.

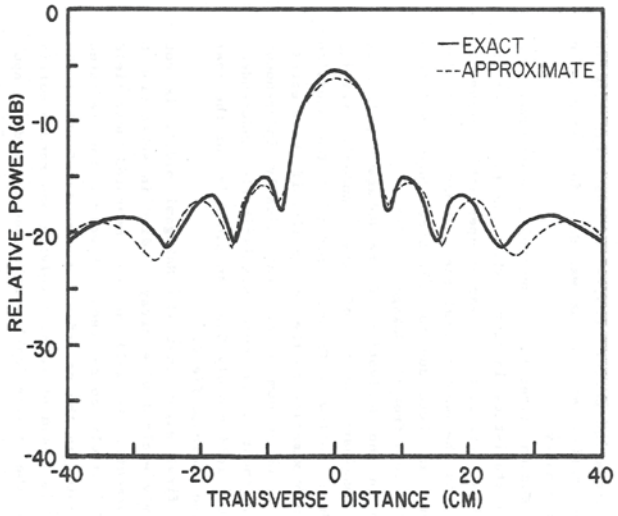

Figure 6. Comparison of exact and retrieved NF Covariance functions $C_{q'q}$ for E(q=0) and E^* at all other NF measurement points.

IV.B.3 STATISTICAL AVERAGE FF PATTERNS

The statistical average power density pattern $\langle P_{ff} \rangle$ is readily computed via Equation (1) by computing the forward Fourier Transforms of the sample average electric field and its complex conjugate and the NF complex covariance functions. The angular brackets signify the statistical average values of the enclosed quantity. The statistical average values for the measured NF quantities are equal to the "sample" average values for these simulations.

$$\left\langle P_{ff}(\omega,\phi)\right\rangle = [0.5\Gamma_o]\left\langle E^*_{ff}(\omega,\phi)E_{ff}(\omega,\phi)\right\rangle + [0.5\Gamma_o]\left\langle E^*_{ff}(\omega,\phi)\right\rangle\left\langle E_{ff}(\omega,\phi)\right\rangle + [0.5\Gamma_o]\left[\sum_{q'}\sum_{q} \underbrace{C_{q'q}}_{NF\ Covar.\ Functions} \exp\left[j\frac{\omega}{c}\sin(\phi)\left(Y_{q'}-Y_q\right)\right]\right] \quad (1)$$

$\left\langle P_{ff}(\omega,\phi)\right\rangle$ = average FF Power Density Pattern,

Γ_o= admittance of free space,

$\omega = 2\pi f$, where f is frequency,

ϕ = FF pattern azimuth angle,

$E_{ff}(\omega,\phi)$= FF electric Field,

$E^*_{ff}(\omega,\phi)$=complex conjugate of $E^*_{ff}(\omega,\phi)$,

where $\left\langle E^*_{ff}(\omega,\phi)\right\rangle\left\langle E_{ff}(\omega,\phi)\right\rangle$ =

$\Sigma_{q'}\Sigma_{q}\left\langle E^*_{q'}(\omega)\right\rangle\left\langle E_q(\omega)\right\rangle \exp\left[j\frac{\omega}{c}\sin(\phi)\left(Y_{q'}-Y_q\right)\right]$

where $\langle\ \rangle$ denote statistical average values,

The statistical average FF power patterns versus FF azimuth angle obtained from Equation 1 for the in-band design frequency of 3.0 GHz and for

the out-out-band pattern at 9.0 GHz are displayed in Figures 7 and 8, respectively. The directivity at the top of all the statistical average FF pattern plots is 21.15 dB above an isotropic radiator.

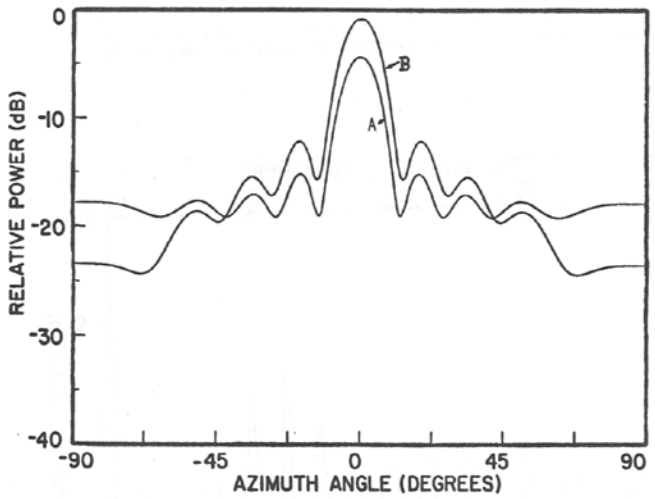

Figure 7. Statistical Average FF Power Density Patterns for randomly-phased wire dipole array of Fig. 1 for the in-band frequency of 3.0 GHz for A=Intrinsic NF covariance functions, and B=Total NF covariance functions

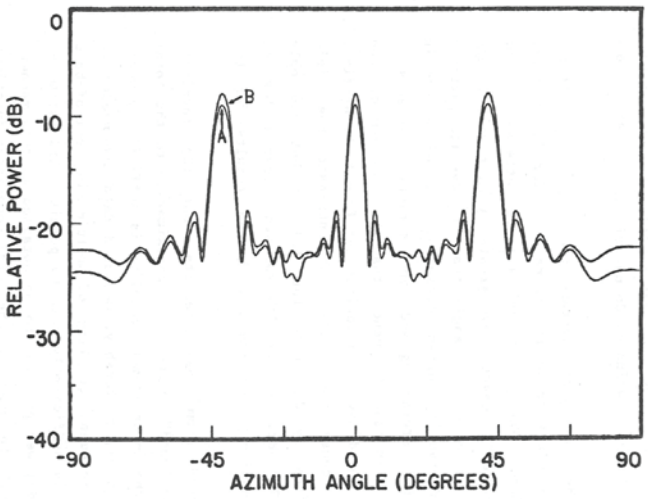

Figure 8. Statistical Average FF Power Density Patterns for randomly-phased wire dipole array of Fig. 1 for the out-of-band frequency of 9.0 GHz, for A=Intrinsic NF covariance functions, and B=Total NF covariance functions.

Each figure contains two plots labeled A and B. The curve labeled B is obtained by transforming the NF data for the case involving the total NF covariance functions while the curve labeled A is for intrinsic NF covariance functions. Note that both Figures 7 and show typical behavior for Statistical Average FF patterns, namely attenuated mainbeam peaks, null filling and raised sidelobe levels with respect to the corresponding quantities for deterministic FF patterns. Further inspection of the plots shows that the differences between the FF Statistical Average Plots for total and intrinsic NF covariance functions are noticeably more significant at the in-band 3.0 GHz than at the out-of- band of 9.0 GHz. This behavior is expected because the mutual coupling effects are correspondingly greater at 3.0 GHz than at 9.0 GHz, as previously noted in the discussion of the NF covariances. The peak magnitude of the Statistical Average FF patterns shown in Figure 5 for 3.0 GHz is about 3.8 dB higher for curve B, as expected due to the mutual coupling effects manifested in curve B.

IV.B.3. Cumulative Probability Distributions

Plots of the Cumulative Probability Distribution are displayed in Figures 9 and 10. Each figure shows the probability that the relative power density is less than or equal to the abscissa. The abscissa in Figure 9 is the relative power density expressed in real numbers, while the abscissa for Figure 10 is the relative power density expressed as decibels. The abscissas were scaled in this manner to illustrate the interesting fact that the cumulative distributions resemble Gaussian distributions when displayed in this manner.

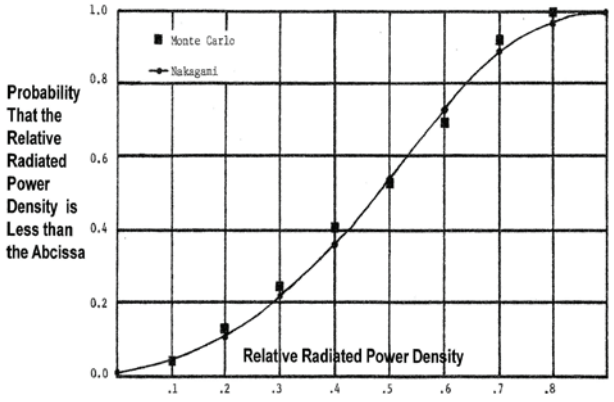

Figure 9. C.P.D. for a mainbeam or grating lobe region for the randomly-phased wire dipole array.

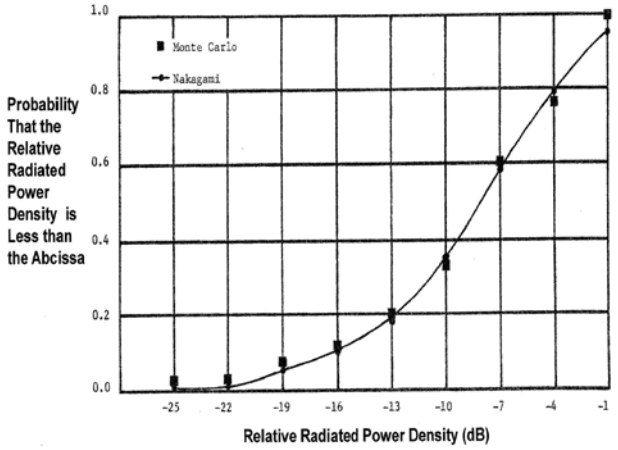

Figure 10. C.P.D. for sidelobe region for the randomly-phased wire dipole array.

We note that FF power density pattern statistics closely follow the Nakagami "m"-Distribution at all relative power density levels for the wire dipole FF patterns examined in this investigation [11,12].

V. CONCLUDING REMARKS

MST probe arrays can be used to great advantage for efficient measurements of NF data for random or non-random electromagnetic fields. MST arrays are scanned electronically along their length and moved mechanically in the orthogonal direction [9]. For example, the total time to acquire the complex fields data over an entire two-dimensional (2-D) planar, cylindrical, or spherical scan surface for a given operational mode of the AUT is typically accomplished in minutes rather than hours. Such speeds are particularly advantageous for situations involving acquisition of random NF data for repeated Monte Carlo Trials. Dual MST probe arrays have been implemented and used for EMC applications by researchers at SUPELEC under the general direction of Prof. Jean-Charles Bolomey to further reduce NF data acquisition times [8,9]. This system employs a novel "clutch" mechanism to allow passage of one of the arrays past the other. This mechanism could possibly be automated and adapted for planar or cylindrical measurement geometries employing dual linear MST probe arrays.

REFERENCES

1. "Statistical Prediction Model for EMC Analysis of Out-of-Band Phased Array Antennas," Barry J. Cown, Fred L. Cain, and Edward F.Duffy, IEEE Transactions on Electromagnetic Compatibility. Vol. EMC-18, No. 4, (November 1976)

2 "Statistical Model for EMC Analysis of Wideband Out-of-Band Phased Arrays," B. J. Cown, Fred L. Cain, E. F. Duffy, 1980 IEEE Electromagnetic Compatibility Symposium Record, (October 1980),

3. "Electromagnetic Models for Antenna Performance, EMC and Biological Effects," IEEE Transactions on Electromagnetic Compatibility, 22, No. 4, (November 1980), invited paper, coauthor

4. 'Near-Field Theory and Techniques for Wideband Radiating Systems at In-Band and Out-of-Band Frequencies, Barry J. Cown and C.E. Ryan, Jr., " Final Technical Report, U. S. Army Contract No. DAAG29-79-C-0029, Project A2179, January 1982, coauthor.

5. "Efficient Measurements and Statistical Analysis of Random Near-Field (NF) Data to Predict Far-Field Pattern Statistics for Wideband Antennas at In-Ban(IB) and Out-of-Band (OB) Frequencies", IEEE AP/URSI Symposium, Orlando, FL, July3-10, 2013, Barry J. Cown, and John P. Estrada.

6. "Antenna Pattem Measurements to Characterize the Out-of-Band Behavior of Reflector Antennas," Final Technical Report, U. S. Army Contract No. FL96 28-80-C-0024, Project A-2548, September 1981, coauthor.

7. 'Far-Field Antenna Performance Investigations Concerning In-Band Effects and Near-Field Structures and Out-of-Band Phased Arrays," Final Engineering Report, Navy Contract N00024-74-C1215, Project A-1613, January 1975, coauthor.

8. "Spherical Near Field Facility for Characterizing Random Emissions", Benoit Fourestie, Jean-Charles Bolomey, Thierry Sarrrebourse, Zwi Altman, and Joe Wiart, IEEE Transactions on Antennas and Propagation, Vol. 53,no 8, 2005, pp 2581-3589.

9. Engineering Applications of the Modulated Scatterer Technique, Jean-Charles Bolomey and Fred E. Gardiol Artech House, Inc., 2001, ISBN 1-58053-147-4.

10. K. Tanabe, "Projection Method for Solving a singular System of Linear Equations and its' Applications", Numerical Mathematics, 17, Springer-Verlag 1971

11. "The m-Distribution—A General formula of Intensity Distribution of Rapid Fading, " Statistical Methods in Radio Wave Propagation", W. C. Hoffman, editor, Pergamon Press, 1963

12. Probability, Random Variables ad Stochastic Processes A. Papoulis and S. Pillai, McGraw Hill, 4th edition, 2002